

THE ‘NO BOUNDARY CONDITION’ OUTFLOW BOUNDARY CONDITION

DAVID F. GRIFFITHS

Department of Mathematics and Computer Science, The University, Dundee DD1 4HN, U.K.

SUMMARY

We use a one-dimensional model problem of advection–diffusion to investigate the treatment recently advocated by Papanastasiou and colleagues to deal with boundary conditions at artificial outflow boundaries.

Using finite elements of degree p , we show that their treatment is equivalent to imposing the condition that the $(p + 1)$ st derivative of the dependent variable should vanish at a point close to the outflow. This is then shown to lead to errors of order $\mathcal{O}((h + 1/Pe)^{p+1})$ in the numerical solutions (where h is the maximum element size and Pe is the global Peclet number), which is superior to the errors of order $\mathcal{O}(h^{p+1} + 1/Pe)$ obtained using a standard no-flux outflow condition. These findings are verified by numerical experiments.

KEY WORDS: advection–diffusion; outflow boundary conditions; finite elements

1. A MODEL PROBLEM IN 1D

We consider the advection–diffusion problem

$$T_t + uT_x = \varepsilon T_{xx} + S \quad (1)$$

on the quarter-plane $\{0 < x < \infty, t > 0\}$, with given initial data $T(x, 0) = T_0(x)$, $0 < x < \infty$, and a Dirichlet boundary condition (BC) at $x = 0$; without loss of generality we may take $T(0, t) = 0$, $t > 0$. We assume that $u(x, t) > 0$ throughout the domain and that ε is a positive constant.

For computational purposes it is necessary to restrict the length of the interval to some finite value L , say. An artificial boundary condition has then to be imposed at $x = L$ (in order to ensure that the truncated problem has a unique solution) in such a way as to not significantly affect the solution in the interior. If it is assumed that the source term $S(x, t)$ and the initial data $T_0(x)$ are such that $T(x, t) \rightarrow \text{constant}$ as $x \rightarrow \infty$ for each $t > 0$ and that L is sufficiently large that the solution is constant in space for $L \leq x < \infty$, then one may impose the ‘no-flux’ condition

$$T_x = 0 \quad \text{at } x = L. \quad (2)$$

This has been the traditional approach. Its success depends not only on L being sufficiently large but also on ε being strictly positive so that any signal is damped as it is convected in the positive x -direction.

Lohéac¹ analyses the effect of imposing an outflow boundary condition on a multidimensional form of equation (1) with $S \equiv 0$. It is proved that a condition of the form

$$T_t + uT_x = 0 \quad \text{at } x = L \quad (3)$$

leads to an error (difference between the problems on the semi-infinite real line and the finite interval $[0, L]$) of order $\mathcal{O}(\varepsilon^2)$ provided that $|u| > 0$. (Our Lemma 1 with $p = 1$ proves a similar result in the steady case.)

The use of extrapolation conditions of the form

$$\frac{\partial^j T}{\partial x^j} = 0 \quad \text{at } x = L \quad (4)$$

for the Navier–Stokes equations is described by Johansson² and Nordström,³ the former recommending the use of $j = 3$ while the latter analyses the case $j = 2$.

We shall analyse a different approach that has recently been proposed by Papanastasiou and colleagues^{4–6} specifically for finite element methods (FEMs). It differs from the methods described above in that it does not seek to impose an outflow BC on the continuous problem but does so implicitly within the discrete approximation of it.

To describe their approach, we require the weak form of equation (1) on the interval $0 < x < L$. This is such that $T(x, t)$ must satisfy the infinite system of ordinary differential equations (ODEs)

$$(\phi, T_t) + (\phi, uT_x) + \varepsilon(\phi_x, T_x) = (\phi, S) + \varepsilon\phi T_x|_{x=L} \quad (5)$$

for all $\phi \in H^1(0, L) \cap \{\phi(0) = 0\}$, together with the given initial data and the boundary condition $T = 0$ at $x = 0$.

If we impose the BC (2), then the boundary term on the right of (5) vanishes, so that

$$(\phi, T_t) + (\phi, uT_x) + \varepsilon(\phi_x, T_x) = (\phi, S), \quad (6)$$

for which (2) is a natural BC.

In contrast with this, Papanastasiou *et al.* suggest that the weak form (5) should be left as it is and that the boundary term should be treated as being unknown—this is termed in Reference 5 a *free boundary condition*. It is our feeling that it should be referred to as the ‘no BC’ boundary condition as this more accurately describes the situation, since within a purely continuous setting (as opposed to finite element approximations) the weak formulation (5) is invalid because it is equivalent to not setting any BC at $x = L$ and the governing equations (5) cannot therefore isolate a unique solution. The aim of this paper is to describe the behaviour of finite element approximations of (5) and, in particular, to ascertain what numerical BCs are implied by this weak form.

In the next section we describe the FE methods and this is followed in Section 3 by the derivation of a boundary condition which is implied by the FE equations. It is shown that finite elements of degree p lead to an outflow BC of the form (4) with $j = p + 1$, except that these hold at some point within the last element rather than at $x = L$. The case $p = 1$ (linear elements) is also equivalent to (3). We also show that for steady problems the new boundary condition leads to errors of order $\mathcal{O}(\varepsilon^{p+1})$ at the outflow when using finite elements of degree p . This contrasts with the errors of order $\mathcal{O}(\varepsilon)$ when using the no-flux condition. These results are verified by a selection of steady and unsteady numerical examples in Section 4.

In Section 5 we avoid the unorthodox implied boundary condition derived in Section 3 by establishing the equivalence of the ‘no BC’ FE equations and the Galerkin FE approximation to a problem with standard Dirichlet–Neumann-type BCs.

2. FE APPROXIMATION

Because there is substantial interest in the p -version as well as the h -version of the FEM, we shall adopt an FE approximation using continuous piecewise polynomials of any degree $p \geq 1$. Our conclusions will be independent of the exact nature of the basis functions employed, but for the sake

of simplicity we assume it to be the classic nodal (or Lagrangian) basis. With the imposition of the BC $T(0, t) = 0$ the dimension of the resulting space is pN . Thus, if we divide the interval $0 < x < L$ into N elements by the knots

$$0 = x_0 < x_1 < \dots < x_N = L,$$

then each element has $p - 1$ nodes in its interior and one node at each of its endpoints. The knots are not required to be equally spaced and we define

$$h = \max_{i \leq j \leq N} (x_j - x_{j-1}), \quad h_N = x_N - x_{N-1}.$$

Denoting the basis functions on this grid by $\{\phi_1, \phi_2, \dots, \phi_{pN}\}$, then the FE approximation T^h to T takes the form

$$T^h(x, t) = \sum_{j=1}^{pN} T_j(t) \phi_j(x), \tag{7}$$

where T_j denotes the value of T^h at the j th node. The FE approximation of (6) then leads to the set of pN ODEs

$$(\phi_j, T_t^h) + (\phi_j, uT_x^h) + \varepsilon(\phi_{j_x}, T_x^h) = (\phi_j, S), \quad j = 1, 2, \dots, pN. \tag{8}$$

On the other hand, the weak form (5) leads to

$$(\phi_j, T_t^h) + (\phi_j, uT_x^h) + \varepsilon(\phi_{j_x}, T_x^h) = (\phi_j, S) + \varepsilon \phi_j T_x^h|_{x=L}, \quad j = 1, 2, \dots, pN. \tag{9}$$

The discrete equations (8) and (9) differ only in the boundary term and consequently the ODEs they generate differ only for the index $j = pN$ associated with nodes lying on the artificial boundary $x = L$. Defining $l = p(N - 1)$, then the nodes in the last element are $x_{l+1}, x_{l+2}, \dots, x_{l+p}$ and the corresponding basis functions $\phi_{l+1}, \phi_{l+2}, \dots, \phi_{l+p}$ are polynomials (rather than piecewise polynomials) on (x_l, L) . Consequently, for $j = l + 1, l + 2, \dots, l + p$, (9) is *exactly* equivalent to

$$\int_{x_l}^L \phi_j (T_t^h + uT_x^h - \varepsilon T_{xx}^h - S) dx = 0, \quad j = l + 1, l + 2, \dots, l + p, \tag{10}$$

which holds for all degrees $p \geq 1$. Note that (10) does not hold for $j < l + 1$.

3. AN IMPLIED BOUNDARY CONDITION

Before turning to finite elements of order p , we look first at the simpler situations of linear ($p = 1$) and quadratic ($p = 2$) elements.

Linear elements

When $p = 1$, we have $T_{xx}^h \equiv 0$ for $x \in (x_l, L)$ and so equations (9) give

$$\int_{x_l}^L \phi_N (T_t^h + uT_x^h - S) dx = 0.$$

Furthermore, since $\phi_N(x) > 0$ for $x \in (x_l, L)$, we may apply the mean value theorem for integrals to deduce that

$$T_t^h + uT_x^h = S \tag{11}$$

at some point $\xi \in (x_l, L)$. Clearly $\xi \rightarrow L$ as $h \rightarrow 0$, so that this may be taken as a form of BC in the neighbourhood of $x=L$. In general ξ varies with t .

If S and u are both linear polynomials in x on the interval (x_l, L) , the point ξ may be identified, since the residual $R \equiv T_t^h + uT_x^h - S$ is then a linear polynomial in x (for each t) which is orthogonal to $\phi_N = (x - x_l)/h_N$ on (x_l, L) . Consequently,

$$R = a(t)(x - L + h_N/3)$$

for some function $a(t)$. Thus $\xi = L - h_N/3$ and the ‘no BC’ boundary condition implies the satisfaction of the ‘reduced equation’ (11) at the fixed location $x = L - h_N/3$. A similar observation has been made by Heinrich and Vionnet,⁷ although they do not identify the point ξ .

Quadratic elements

When $p=2$, we have $T_{xx}^h \equiv \text{constant}$ for $x \in (x_l, L)$ and (10) holds for $j = l + 1, l + 2$ —there are two discrete equations pertaining to the element (x_l, L) . We shall assume that u and S are polynomials of degree one and two in x respectively on (x_l, L) whose coefficients may depend on t .

Since R is a polynomial of degree two in x that is orthogonal on (x_l, L) to both ϕ_{l+1} and ϕ_{l+2} , it must therefore be orthogonal to all polynomials of degree two that vanish at the left endpoint $x = x_l$ of the outflow element. It follows that

$$R = a(t)(5X^2 - 2X - 1), \quad X = -1 + 2\frac{x - x_l}{h_N},$$

where a is some function of t alone (different from that in the linear case). Thus the residual must be zero at the two points $x = \xi_1, \xi_2 \in (x_l, L)$, where

$$\xi_{1,2} = x_l + h_N(1/5 \pm \sqrt{6/10}).$$

In contrast with the linear case, these conditions do not provide BCs for the system but merely show that the differential equation (1) is exactly satisfied at these points—the residual is collocated at $x = \xi_1$ and $x = \xi_2$. However, using the facts that $\partial R/\partial x = 0$ at $X = 1/5$ and $T_{xx}^h \equiv \text{constant}$ on (x_l, L) , it follows that

$$\left. \frac{\partial}{\partial x} (T_t^h + uT_x^h - S) \right|_{x=\xi} = 0 \tag{12}$$

at $x = \xi = x_l + 3h_N/5$. This condition is independent of the PDE (1) and may therefore be construed as being the BC implied by (9).

An alternative derivation of a slightly weaker result may be given for the cases where S is not necessarily a quadratic polynomial or where u is not linear in x . We begin by scaling the basic functions to have ‘unit mass’:

$$\hat{\phi}_j(x) = \phi_j(x) / \int_0^L \phi_j(t) dt, \quad j = l + 1, l + 2; \tag{13}$$

then clearly the FE equations (8)–(10) continue to hold with ϕ_j replaced by $\hat{\phi}_j$. Subtracting the two resulting equations corresponding to $j = l + 1, l + 2$ from each other gives (using $T_{xx}^h \equiv \text{constant}$ on (x_l, L))

$$(\hat{\phi}_{l+1} - \hat{\phi}_{l+2}, T_t^h + uT_x^h - S) = 0. \tag{14}$$

Defining $\psi(x) = \int_{x_l}^x (\hat{\phi}_{l+1}(t) - \hat{\phi}_{l+2}(t)) dt$, then it is readily verified that

$$\psi(x) = 6X^2(1 - X), \quad X = (x - x_l)/h_N.$$

Thus $\psi(x_l) = \psi(L) = 0$ and integrating (14) by parts leads to

$$\left(\psi, \frac{\partial}{\partial x} (T_t^h + uT_x^h - S) \right) = 0. \tag{15}$$

Furthermore, since $\psi(x) > 0$ for $x \in (x_l, L)$, we may again apply the mean value theorem for integrals to conclude that (12) holds. This argument does not identify the precise location of $\xi \in (x_l, L)$, but if we assume that S and u are sufficiently smooth, it may be shown that $\xi = L - 2h_N/5 + \mathcal{O}(h^2)$, so that the former result is essentially recovered.

General case

We return now to the case of finite elements of general degree $p \geq 1$ and establish the following result.

Theorem 1

If T^h is an FE function of the form (7) and R denotes the corresponding residual

$$R(x, t) \equiv T_t^h + uT_x^h - \varepsilon T_{xx}^h - S, \quad x \in (x_l, L), \tag{16}$$

then the ‘no BC’ FE equations (9) imply that for each $t > 0$ there is a point $\xi \in (x_l, L)$ where

$$\frac{\partial^{p-1}}{\partial x^{p-1}} (T_t^h + uT_x^h - S) \Big|_{x=\xi} = 0. \tag{17}$$

Furthermore, if S is a polynomial in x of degree $\leq p$ and if u is a linear polynomial in x for $x \in (x_l, L)$ and for each $t > 0$, then

- (i) the BC (17) holds at $\xi = L - [p/(2p + 1)]h_N$
- (ii) the residual is zero at the p zeros $\{\xi_k\}$ of the Radau polynomial of degree p on (x_l, L) . That is, the finite element equations in the ‘outflow element’ imply

$$R(\xi_k, t) = 0, \quad k = 1, 2, \dots, p, \tag{18}$$

so that they are equivalent to collocation at the Radau points in this element.

Remarks

1. The assumption made in the second part of Theorem 1 that $S(x, t)$ be a polynomial in x of degree not exceeding p in (x_l, L) will be met if one adopts the common practice of projecting the source terms onto the underlying finite element basis in order to facilitate the evaluation of integrals.
2. With less restrictive conditions on S and u , e.g. that their $(p + 1)$ st and second derivatives respectively with respect to x be continuous for $x \in (x_l, L)$, one can show that the ‘boundary condition’ (17) holds at

$$\xi = L - \frac{p}{2p + 1} h_N + \mathcal{O}(h^2).$$

3. The Radau polynomial $r_p(x)$ of degree p on (x_l, L) is defined by (see e.g. the book by Davis and Rabinowitz⁸)

$$r_p(x) = \frac{P_{p+1}(X) + P_p(X)}{1 + X}, \quad X = -1 + 2\frac{x - x_l}{h_N}, \quad x \in (x_l, L),$$

where $P_n(X)$ denotes the n th-degree Legendre polynomial for $X \in (-1, 1)$.

4. It is interesting to note that the point ξ at which (17) holds and the collocation points $\{\xi_k\}$ are stationary for all time (to $\mathcal{O}(h^2)$ in the general case).

Proof of Theorem 1

The proof depends on the polynomial

$$\psi(x) = (1 + X)^p(1 - X)^{p-1}, \tag{19}$$

where, here and throughout the proof, x and X are related by

$$X = -1 + 2\frac{x - x_l}{h_N}, \tag{20}$$

a linear map from $x \in (x_l, L)$ to $X \in (-1, 1)$.

We first note that $\partial^{(p-1)}\psi/\partial x^{(p-1)}$ is a polynomial of degree p that vanishes at $x = x_l (X = -1)$. Consequently, there are coefficients $\{a_1, a_2, \dots, a_p\}$ such that

$$\frac{\partial^{p-1}\psi}{\partial x^{p-1}}(x) = \sum_{j=1}^p a_j \phi_{j+l}(x),$$

and by multiplying the $(j - l)$ th equation of (10) by a_j and summing, we find that

$$\int_{x_l}^L \frac{\partial^{p+1}\psi}{\partial x^{p-1}}(T_t^h + uT_x^h - \varepsilon T_{xx}^h - S)dx = 0. \tag{21}$$

We next note that the polynomials

$$\psi(x), \quad \frac{\partial^k \psi}{\partial x^k}(x), \quad k = 1, 2, \dots, p - 2,$$

all vanish at both $x = x_l$ and $x = L$. Thus, when we integrate (21) by parts $p - 1$ times, we obtain

$$\int_{x_l}^L \psi \frac{\partial^{p-1}}{\partial x^{p-1}}(T_t^h + uT_x^h - \varepsilon T_{xx}^h - S)dx = 0.$$

Now, since T^h is a polynomial of degree p , its $(p + 1)$ st derivative is identically zero, so that this reduces to

$$\int_{x_l}^L \psi \frac{\partial^{p-1}}{\partial x^{p-1}}(T_t^h + uT_x^h - S)dx = 0, \tag{22}$$

and since $\psi(x) > 0$ for $x \in (x_l, L)$, we invoke the mean value theorem for integrals to deduce that (17) holds at some point $\xi \in (x_l, L)$.

When u is a linear function and S is a polynomial of degree p , the second factor in the integrand of (22) is a linear polynomial so we may express it in the form

$$\frac{\partial^{p-1}}{\partial x^{p-1}}(T_t^h + uT_x^h - S) = A(B - X).$$

Substituting this into (22), using the definition of ψ and evaluating the resulting integrals gives

$$B = \int_{-1}^1 X\psi(X)dX / \int_{-1}^1 \psi(X)dX,$$

so that

$$B = \frac{p + 1}{2p + 1}.$$

Thus we have a zero at $X = B$ which, through (20), leads to $\xi = L - ph_N/(2p + 1)$ as required.

The proof of part (ii) of the theorem depends on the observation that the residual R is a polynomial of degree p that, by (10), is orthogonal to all polynomials of degree p which vanish at $x = x_l$ (because of this last condition, there is one less degree of freedom than would be required to ensure that R were identically zero). Consequently, R must be a multiple of the Radau polynomial of degree p .⁸

$$R(x, t) = a(t)r_p(x), \quad x \in (x_l, L),$$

for some function $a(t)$, and therefore (18) must hold. □

It follows from Theorem 1 that the ‘no BC’ finite element equations provide an approximation to the non-standard problem consisting of (1) on the interval $0 < x \leq \xi$, a Dirichlet condition at $x = 0$ and the boundary condition

$$\frac{\partial^{p-1}}{\partial x^{p-1}}(T_t + uT_x - S) = 0 \quad \text{at } x = \xi$$

for some $\xi = \xi(h, t) \in (x_l, L)$. When u and S are sufficiently smooth, the differential equation may be used to simplify the boundary condition at the outflow and this leads to the initial boundary value problem (IBVP)

$$\begin{aligned} T_t + uT_x &= \varepsilon T_{xx} + S, & 0 < x \leq \xi, \\ T(0, t) &= 0, & t > 0, \\ \frac{\partial^{p+1} T}{\partial x^{p+1}}(\xi, t) &= 0, & t > 0. \end{aligned} \tag{23}$$

Discrete versions of this outflow boundary condition have been discussed in the finite difference literature on hyperbolic problems ($\varepsilon = 0$)^{9,10} and also in the context of the Navier–Stokes equations.^{2,3}

We shall demonstrate through numerical experiments in Section 4 that the solutions of the ‘no BC’ finite element method do indeed converge to those of problem (23), so we may interpret the solutions of (23) as describing the properties of equations (9). We therefore need to quantify how far the solutions of (23) lie from those to the original problem posed on $0 < x < \infty$. We shall consider this issue in the next subsection.

3.1. Stationary problems

Our aim is to determine the difference between the solution to the problem

$$\mathcal{G}^\infty \begin{cases} uT_x = \varepsilon T_{xx} + S, & 0 < x \leq \infty, \\ T(0) = 0, \\ T(x) \rightarrow \text{constant}, & x \rightarrow \infty, \end{cases} \tag{24}$$

denoted by T^∞ , and that of

$$\mathcal{S}^\xi \begin{cases} uT_x = \varepsilon T_{xx} + S, & 0 < x \leq \xi, \\ T(0) = 0, \\ \frac{\partial^k T}{\partial x^k}(\xi) = 0, \end{cases} \tag{25}$$

which we denote by T^ξ . If u is constant, then the general solution of $uT_x = \varepsilon T_{xx} + S$ satisfying $T(0) = 0$ is given by

$$T(x) = A(e^{ux/\varepsilon} - 1) + \frac{1}{u} \int_0^x S(s) ds - \frac{1}{u} \int_0^x e^{u(x-s)/\varepsilon} S(s) ds \tag{26}$$

for any constant A .

If $e^{-ux/\varepsilon} \int_0^x S(s) ds \rightarrow 0$ as $x \rightarrow \infty$, then $T(x) \rightarrow \text{constant}$ if the constant A is chosen such that $A = A_\infty$, where

$$A_\infty = \int_0^\infty e^{-us/\varepsilon} S(s) ds.$$

This together with (26) defines T^∞ .

The difference $e \equiv T^\infty - T^\xi$ satisfies the homogeneous differential equation $-\varepsilon e'' + ue' = 0$ with $e(0) = 0$ and $d^k e/dx^k = d^k T^\infty/dx^k$ at $x = \xi$. Consequently,

$$e(x) = \left(\frac{\varepsilon}{u}\right)^k \frac{d^k T^\infty}{dx^k}(\xi) (e^{u(\xi-x)/\varepsilon} - e^{u\xi/\varepsilon})$$

for $0 \leq x \leq \xi$. It is readily shown that

$$\frac{d^k T^\infty}{dx^k}(\xi) = \frac{1}{\xi} \int_\xi^\infty e^{u(\xi-s)/\varepsilon} \frac{d^{k-1} S}{ds^{k-1}}(s) ds.$$

These results lead to the following lemma.

Lemma 1

If u is constant and S and its first $k - 1$ derivatives are continuous and bounded on $(0, \infty)$, then the solutions to problems \mathcal{S}^∞ and \mathcal{S}^ξ differ by

$$T^\infty(x) - T^\xi(x) = \frac{1}{u} \left(\frac{\varepsilon}{u}\right)^{k-1} \int_0^\infty e^{-us/\varepsilon} \frac{d^{k-1} S}{ds^{k-1}}(s + \xi) ds (e^{-u(\xi-x)/\varepsilon} - e^{-u\xi/\varepsilon}) \tag{27}$$

for $0 \leq x \leq \xi$. Thus

$$\max_{0 \leq x \leq \xi} |T^\infty(x) - T^\xi(x)| \leq \frac{1}{u} \left(\frac{\varepsilon}{u}\right)^k \max_{\xi \leq x \leq \infty} \left| \frac{d^{k-1} S}{dx^{k-1}}(x) \right| \tag{28}$$

and the maximum of the left-hand side is achieved at $x = \xi$.

Remarks

1. The smoothness requirements on the source term S may be weakened (except in the neighbourhood of $x = \xi$) at the expense of introducing additional exponentially small terms into the right sides of (27) and (28).

2. The requirement of u being constant may be relaxed (subject to $u(x) > 0$) at the expense of introducing more complex integrating factors. The results given are valid only if $u \neq 0$, so that some element of convection is essential in the problem.
3. The most significant conclusion is that the higher the order of derivative boundary condition imposed at $x = \xi$, the closer the solutions T^∞ and T^ξ lie to each other. If the no-flux condition (2) is imposed, we have $\xi = L, k = 1$ and a difference of $\mathcal{O}(\varepsilon)$, but with linear ($k = p + 1 = 2$) and quadratic ($k = p + 1 = 3$) elements in the 'no BC' formulation we get differences of $\mathcal{O}(\varepsilon^2)$ and $\mathcal{O}(\varepsilon^3)$ respectively (the first of these may be deduced as a special case of the results of Lohéac¹). Moreover, the last factor on the right of (27) represents a term that is exponentially small outside a boundary layer of width $\mathcal{O}(\varepsilon)$ at $x = \xi$; any differences are therefore confined to this layer.
4. If the time-dependent problem (23) achieves a steady state as $t \rightarrow \infty$, then the results of Lemma 1 also hold in that case for large times.

4. NUMERICAL RESULTS

We present three examples designed to confirm the results of the preceding sections.

Example 1. Steady problem

We choose $u = 1$ and consider the problem \mathcal{S}^∞ with

$$S(x) = \begin{cases} \sin(x), & 0 \leq x \leq \pi, \\ 0, & \pi < x < \infty. \end{cases}$$

The solutions T^∞ are shown in Figure 1 for $\varepsilon = 0.1$ (broken line) and $\varepsilon = 0.01$ (full line).

We solve the problem on the truncated domain with $L = 1$ using both the no-flux formulation (8) and the 'no BC' formulation (9) with linear and quadratic elements. The choices of L and u may be compensated for by rescaling x, ε and S . In all cases we use $\varepsilon = 1, 0.1, 0.01, 0.001$ and a uniform grid in space with $h = 2^{-j}, j = 2, 3, \dots, 10$. The computations were carried out in Matlab on a Sun SPARCstation LX.

The solutions for linear elements with $h = 1/32$ are shown in Figure 2: (a) $\varepsilon = 1$, (b) $\varepsilon = 0.1$, (c) $\varepsilon = 0.01$ and (d) $\varepsilon = 0.001$. The full line denotes the solution T^∞ , the crosses denote the solution using 'no BC' at $x = 1$ and the circles denote the solution using the no-flux boundary condition (2). The 'no BC' condition is seen to be effective even at very large values of the diffusion coefficient and is generally superior to the no-flux condition.

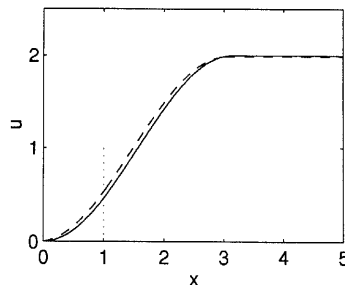


Figure 1. Solution T^∞ to Example 1 with $\varepsilon = 0.1$ (broken line) and $\varepsilon = 0.01$ (full line). The vertical dotted line shows the location of the fictitious boundary

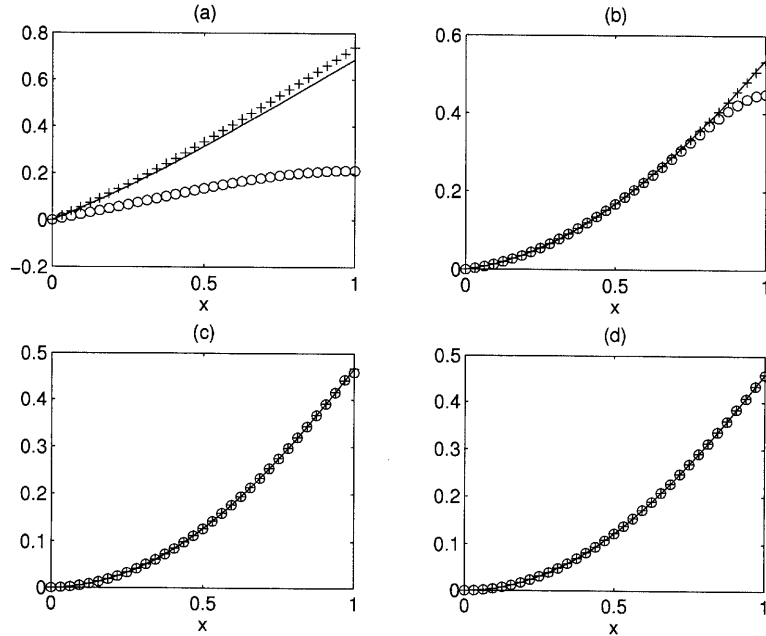


Figure 2. T^∞ (full line), T_{noflux}^h (circles) and T_{nobc}^h (crosses) for Example 1 with $h = 1/32$ and (a) $\varepsilon = 1$, (b) $\varepsilon = 0.1$, (c) $\varepsilon = 0.01$, (d) $\varepsilon = 0.001$

Each part of Figure 3 shows a log–log plot of the difference between a reference solution and a computed solution (evaluated at $x = 1 - h$) as a function of h for $\varepsilon = 1$ (crosses), $\varepsilon = 0.1$ (circles), $\varepsilon = 0.01$ (asterisks) and $\varepsilon = 0.001$ (full line). In Figure 3(a) we show $T^\infty - T_{\text{noflux}}^h$, where T_{noflux}^h is determined using equations (8). It is clear that as $h \rightarrow 0$ the difference is proportional to ε , in accordance with Lemma 1 with $k = 1$. Figure 3(b) shows the difference $T^\infty - T_{\text{nobc}}^h$ between the exact solution to the problem on the unbounded domain and that produced by the linear ‘no BC’ formulation. For small values of ε the difference behaves as $\mathcal{O}(h^2)$ but asymptotes as $h \rightarrow 0$ to a value proportional to $\mathcal{O}(\varepsilon^2)$, again in accordance with Lemma 1, this time with $k = p + 1 = 2$.

Figures 3(c) and 3(d) compare the difference between T_{nobc}^h and T^ξ , where, from Theorem 1, $\xi = 1 - h/3$. In Figure 3(c) the difference tends to zero with h , but the rate of convergence, although close to two for larger values of h , ultimately diminishes to $\mathcal{O}(h)$. It is seen in Theorem 1 that the precise location of ξ is only known when S has the same degree as the underlying FE space. Accordingly, we also compute the ‘no BC’ FEM with S replaced by its interpolant S^h defined by

$$S^h(x) = \sum_{j=0}^N S(x_j)\phi_j(x).$$

The resulting difference $T^\xi - T_{\text{nobc}}^h$ is shown in Figure 3(d) and is seen to converge optimally at $\mathcal{O}(h^2)$.

The results of exactly analogous computations using quadratic finite elements are shown in Figure 4. They are again in agreement with the results of Theorem 1 (with $p = 2$, $\xi = 1 - 2h/5$) and Lemma 1 with $k = p + 1 = 3$.

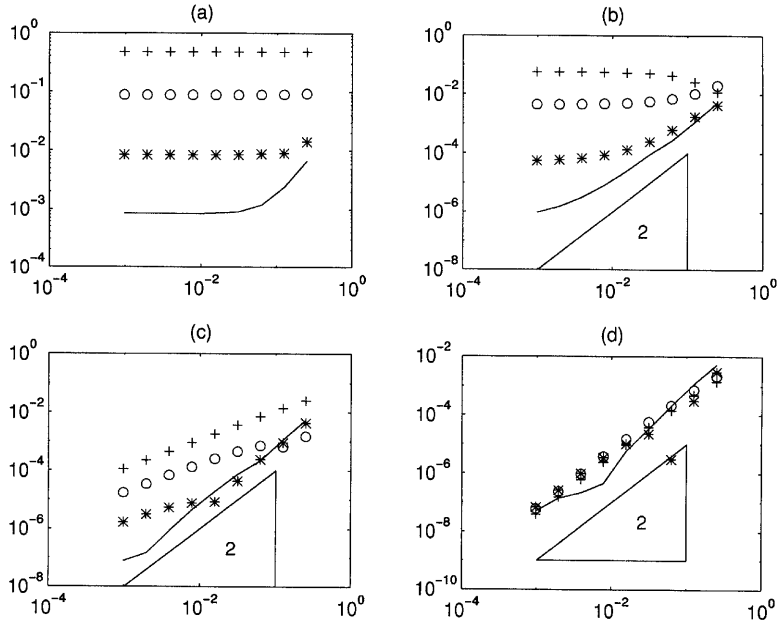


Figure 3. Example 1 with linear elements: (a) $T^\infty - T^h_{\text{no flux}}$, (b) $T^\infty - T^h_{\text{nbc}}$, (c) $T^\xi - T^h_{\text{nbc}}$ and (d) $T^\xi - T^h_{\text{nbc}}$ (with source term interpolated) as h varies. Key: crosses, $\epsilon = 1$; circles, $\epsilon = 0.1$; asterisks, $\epsilon = 0.01$; full line, $\epsilon = 0.001$

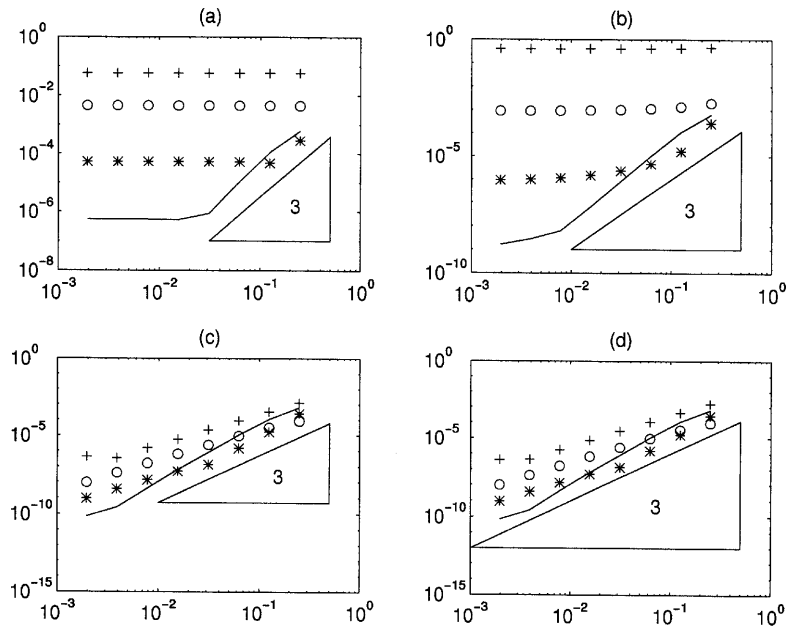


Figure 4. As for Figure 3 but using quadratic elements

Example 2. Unsteady problem

This example is designed to test the assertion that the solutions of the ‘no BC’ equations (9) converge to those of the IBVP (23) as $h \rightarrow 0$. We choose initial data so as to give an exact solution of equations (23) with $L = 1, u = 1$ and $S = 0$. The initial data are dependent on the degree p , the location $\xi = 1 - ph/(2p + 1)$ and, consequently, on h . The exact solution is chosen as

$$T(x, t) = \frac{2}{\varepsilon} e^{(x-1)/2\varepsilon} \sum_{j=1,2} (-1)^{j-1} \frac{\sin(\gamma_j x)}{\sin(\gamma_j)} e^{-(1-4\gamma_j^2 \varepsilon t)/4\varepsilon}, \tag{29}$$

which satisfies $T(0, t) = 0, T(1, 0) = 0$ and also the boundary condition $\partial^{p+1}T/\partial x^{p+1} = 0$ at $x = \xi$ if γ_1 and γ_2 are roots of

$$(1 - 4\varepsilon^2 \gamma^2) \sin(\gamma \xi) + 4\varepsilon \gamma \cos(\gamma \xi) = 0, \quad \xi = 1 - h/3, \quad p = 1, \tag{30}$$

$$(1 - 12\varepsilon^2 \gamma^2) \sin(\gamma \xi) + 2\varepsilon \gamma (3 - 4\varepsilon^2 \gamma^2) \cos(\gamma \xi) = 0, \quad \xi = 1 - 2h/5, \quad p = 2. \tag{31}$$

We choose the two smallest positive roots of these equations. The solutions are shown in [Figure 5](#) for $p = 1, h = 1/64$ and $\varepsilon = 0.1$ (left) and $\varepsilon = 0.01$ (right). The presence of a boundary layer at $x = 1$ is evident for $\varepsilon = 0.01$. The solutions have a qualitatively similar form for $p = 2$.

The solution (29) defines initial data

$$T_0(x) = \frac{2}{\varepsilon} e^{(x-1)/2\varepsilon} \sum_{j=1,2} (-1)^{j-1} \frac{\sin(\gamma_j x)}{\sin(\gamma_j)}$$

for $0 < x < 1$, and by extending this to be zero outside the interval, we may construct a solution of (1) on the entire real line by

$$T^\infty(x, t) = \frac{1}{\sqrt{4\pi \varepsilon t}} \int_0^1 T_0(s) e^{-(x-s-t)^2/4\varepsilon t} ds.$$

when ε is small, $T^\infty(0, t)$ is exponentially small and so this expression is sufficiently close to the solution that satisfies $T(0, t) = 0$.

In the numerical results that we present, the time integration of equations (9) has been accomplished using a Matlab code based on variable order, variable step, backward differentiation formulae and controls the level of local errors in time to a user-specified tolerance. We have used a tolerance of 10^{-7} in our computations.

[Figure 6](#) shows the solutions using linear elements at $t = \varepsilon$ with $h = 1/64$ and (a) $\varepsilon = 0.1$ and (b) $\varepsilon = 0.01$ (only the solution in the interval $0.75 \leq x \leq 1$ is shown). The circles denote the solution T_{noflux}^h , the crosses denote T_{nobc}^h , the full line denotes T given by (29) and the dotted line denotes T^∞ . There is very close agreement between T_{nobc}^h and T in both cases, whereas there is a notable discrepancy between T_{noflux}^h and both T and T^∞ .

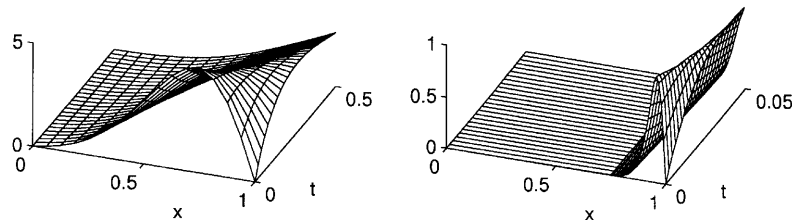


Figure 5. Example 2: Exact solutions of IBVP (23) with $p = 1, h = 1/64$ and $\varepsilon = 0.1$ (left) and $\varepsilon = 0.01$ (right)

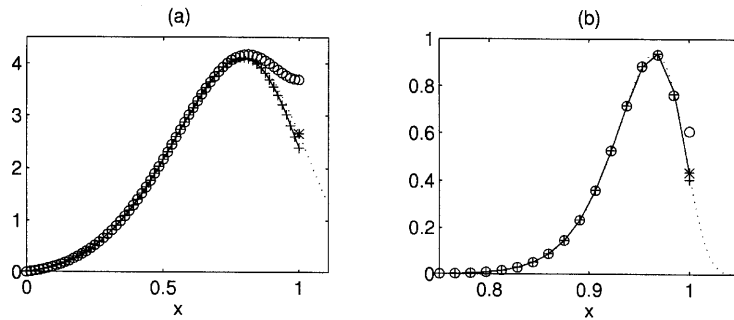


Figure 6. Example 2: solutions using linear elements at $t = \varepsilon$ with $h + 1/64$ and (a) $\varepsilon = 0.1$ and (b) $\varepsilon = 0.01$ (only solution in interval $0.75 \leq x \leq 1$ is shown). Key; circles, T^h_{noflux} ; crosses, T^h_{nobc} ; full line, T ; dotted line, T^∞

The corresponding results for quadratic elements are shown in Figure 7. The conclusions to be drawn are the same as for linear elements.

Quantitative measures of the differences $T^\infty - T^h_{\text{noflux}}$, $T^\infty - T^h_{\text{nobc}}$ and $T - T^h_{\text{nobc}}$ as functions of h are presented in Figure 8 (Linear) and Figure 9 (quadratic). Results are given for $\varepsilon = 0.1$ (circles) and $\varepsilon = 0.01$ (crosses). It is seen that both $T^\infty - T^h_{\text{noflux}}$ (Figures 8(a) and 9(a)) and $T^\infty - T^h_{\text{nobc}}$ (Figures 8(b) and 9(b)) behave as $\mathcal{O}(\varepsilon)$ as $h \rightarrow 0$ whereas $T - T^h_{\text{nobc}}$ (Figure 8(c) and 9(c)) behaves as $\mathcal{O}(h^2)$ for both linear and quadratic elements, suggesting that the solutions of the ‘no BC’ FE equations do indeed converge to those of (23).

This example does not properly reflect the ability of the various FE methods to approximate T^∞ because of the boundary layer in the neighbourhood of $x = 1$. We therefore include one further example which does not contain any such layers.

Example 3. Convection of a Gaussian

We require a smooth exact solution T^∞ on $0 < x < \infty$ and this is taken to be

$$T^\infty(x, t) = \frac{1}{\sqrt{4\pi\varepsilon(t + t_0)}} e^{-(x-x_0-t)^2/4\varepsilon(t+t_0)}$$

with $t_0 = 0.1$ and two choices of ε and x_0 . For $\varepsilon = 0.1$ we take $x_0 = 0.5$ and integrate over $0 < t < 1$, whereas for $\varepsilon = 0.01$ we take $x_0 = 0.75$ and integrate over $0 < t < 0.4$. These have been chosen so that the major features of the solution are convected out of the domain in the specified time intervals. The solutions are shown in Figure 10 with $\varepsilon = 0.1$ (left) and $\varepsilon = 0.01$ (right).

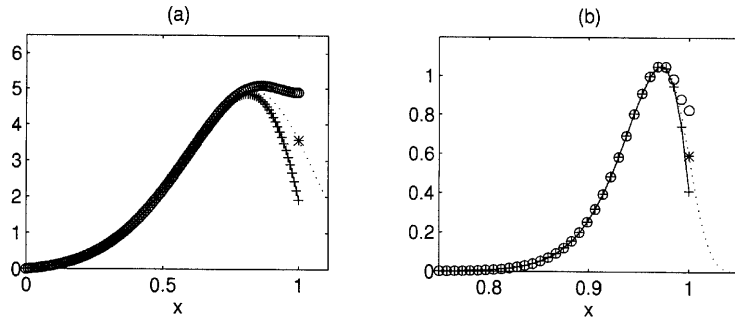


Figure 7. As for Figure 6 but using quadratic elements

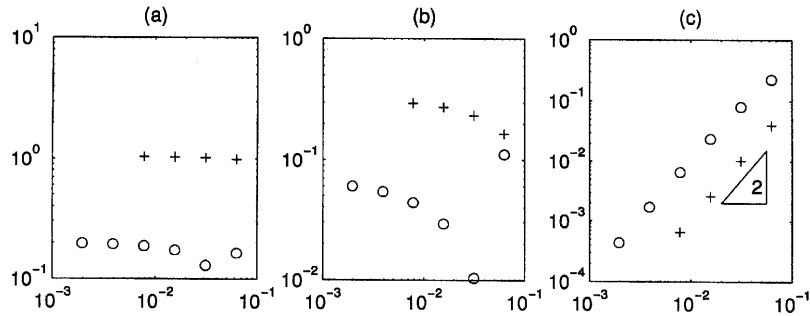


Figure 8. Example 2 with linear elements: (a) $T^\infty - T^h_{\text{noflux}}$, (b) $T^\infty - T^h_{\text{nobc}}$ and (c) $T - T^h_{\text{nobc}}$ against h for $\varepsilon = 0.1$ (crosses) and $\varepsilon = 0.01$ (circles)

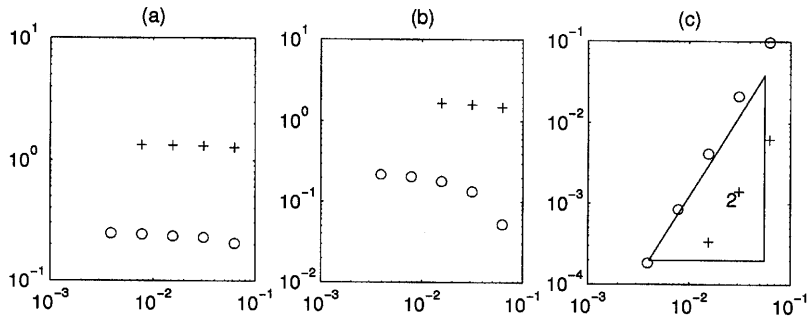


Figure 9. As for Figure 8 but using quadratic elements

The grids have used $h = 1/32$ for linear elements and $h = 1/16$ for quadratic elements (so that both systems have the same number of degrees of freedom). Reducing the size of h in both cases leads to virtually identical results (to graphical accuracy), since the dominant factor in the error is the value of ε .

The solutions at the outflow boundary $x = 1$ for linear elements are shown in Figure 11(a) for $\varepsilon = 0.1$ and Figure 11(b) for $\varepsilon = 0.01$. The circles, crosses and full line denote the solutions T^h_{noflux} , T^h_{nobc} and T^∞ respectively. For both values of ε the ‘no BC’ formulation is clearly superior to the no-flux boundary conditions.

The corresponding results for quadratic elements are shown in Figure 12. The magnitude of the errors in T^h_{noflux} is comparable with that for linear elements in each case. The ‘no BC’ formulation shows a marginal improvement over the use of linear elements.

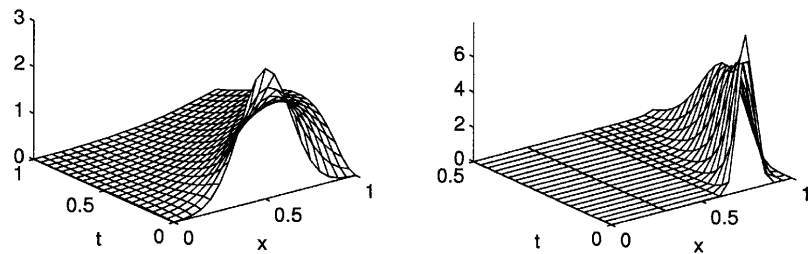


Figure 10. Example 3: exact solutions with $\varepsilon = 0.1$ (left) and $\varepsilon = 0.01$ (right)

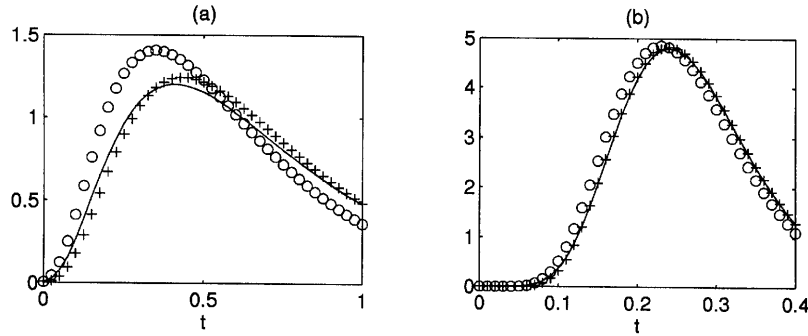


Figure 11. Example 3: solutions using linear element at $x = 1$ with $h = 1/32$ and (a) $\varepsilon = 0.1$ and (b) $\varepsilon = 0.01$. Key: circles, T_{noflux}^h ; crosses, T_{nobc}^h ; full line, T^∞

5. AN EQUIVALENT DIRICHLET-NEUMANN PROBLEM

It was shown in Section 3 that the ‘no BC’ finite element equations (9) approximate the IBVP (23) in which there features a boundary condition involving the $(p + 1)$ st derivative of T . This leads to a non-standard problem for which no theory has been developed regarding either convergence or, in steady cases, whether the linear equations they generate are non-singular. We shall show that this difficulty may be partially circumvented by relating the ‘no BC’ finite element equations to the standard Galerkin FE approximation of a more standard problem. The process will be sketched for FE spaces of arbitrary degree p and details given for the cases $p = 1$ and 2 .

We begin with some preliminary results that will enable us to determine a combination of test functions to replace ϕ_{pN} in (9) so that the ‘no BC’ equations may be reorganized to resemble those for a Dirichlet-Neumann problem. For each p let Ψ denote a polynomial of degree $2p$ (which we shall specify below) and define

$$\psi(x) = \frac{d^p \Psi}{dx^p}(x). \tag{32}$$

Then, if $V^h = \sum_1^{pN} V_j^h \phi_j(x)$ denotes an arbitrary finite element function, it may be shown by integrating by parts that

$$\int_{x_l}^L \psi(-\varepsilon V_{xx}^h + u V_x^h) dx = u \frac{\partial^{p-1} \Psi}{\partial x^{p-1}} V_x^h \Big|_{x=x_l}^L - \sum_{j=2}^p (-1)^j \frac{\partial^j V^h}{\partial x^j} \left(\varepsilon \frac{\partial^{p-j+1} \Psi}{\partial x^{p-j+1}} + u \frac{\partial^{p-j} \Psi}{\partial x^{p-j}} \right) \Big|_{x=x_l}^L.$$

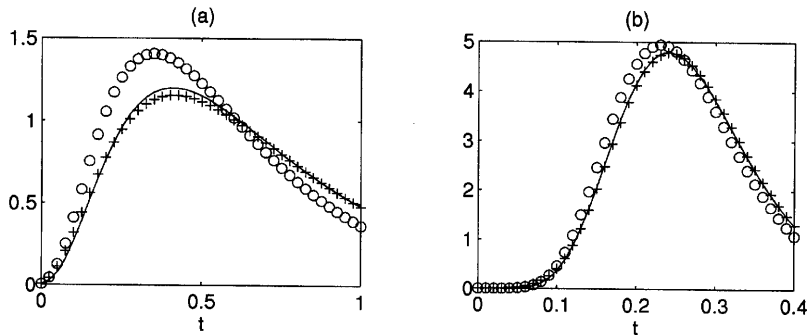


Figure 12. As for Figure 11 but using quadratic elements

We now impose the $2p + 1$ interpolation conditions

$$\begin{aligned} \frac{d^j \Psi}{dx^j}(x_l) &= 0, \quad j = 0, 1, \dots, p, \\ \frac{d^{p-j} \Psi}{dx^{p-j}}(L) &= (-1)^{j+1} \left(\frac{\varepsilon}{u}\right)^j, \quad j = 1, 2, \dots, p, \end{aligned}$$

which uniquely define $\Psi(x)$, and we obtain

$$\int_{x_l}^L \psi(-\varepsilon V_{xx}^h + u V_x^h) dx = \varepsilon V_x^h(L). \quad (33)$$

Moreover, since $\psi(x)$ is a polynomial of degree p on (x_l, L) with $\psi(x_l) = 0$, there are coefficients $\{a_j\}$ such that

$$\psi(x) = \sum_{j=1}^p a_j \phi_{j+l}(x),$$

a linear combination of the FE basis functions $\{\phi_j\}$ whose support is restricted to the outflow element (x_l, L) .

The essential features are contained in the steady case and so we set all time derivatives to zero—we will subsequently return to the unsteady case. Multiplying the j th equation of (10) by a_j , summing over j and adding the result to the last equation of (10), we obtain, since $p + l = pN$,

$$\int_{x_l}^L (\phi_{pN} + \psi)(u T_x^h - \varepsilon T_{xx}^h - S) dx = 0.$$

Reorganizing this and using (33) with $V^h = T^h$, we find

$$\int_{x_l}^L \phi_{pN} (u T_x^h - \varepsilon T_{xx}^h - S) dx + \varepsilon T_x^h(L) = \int_{x_l}^L \psi S dx.$$

We now integrate the second-derivative term by parts and use $\phi_{pN}(L) = 1$ to give

$$\int_{x_l}^L (\phi_{pN} u T_x^h + \varepsilon \phi_{pN_x} T_x^h - \phi_{pN} S) dx = \int_{x_l}^L \psi S dx. \quad (34)$$

Since $\phi_j(L) = 0, j = 1, 2, \dots, pN - 1$, we have now shown that the steady ‘no BC’ finite element equations (9) are equivalent to

$$\begin{aligned} (\phi_j, u T_x^h) + \varepsilon (\phi_{j_x}, T_x^h) &= (\phi_j, S), \quad j = 1, 2, \dots, pN - 1, \\ (\phi_j, u T_x^h) + \varepsilon (\phi_{j_x}, T_x^h) &= (\phi_j, S) + \int_{x_l}^L \psi S dx, \quad j = pN. \end{aligned}$$

This is the standard Galerkin FE approximation of the Dirichlet–Neumann problem

$$\begin{aligned} -\varepsilon T_{xx} + u T_x &= S, \quad 0 < x < L, \\ T(0) &= 0, \\ u T_x(L) &= \alpha, \end{aligned} \quad (35)$$

where

$$\alpha = \frac{u}{\varepsilon} \int_{x_l}^L \psi S ds$$

clearly depends on h .

For linear elements it is readily shown that $\psi = 2\varepsilon(x - x_l)/uh_N^2$ and, by Taylor expansions,

$$\begin{aligned} \alpha &= S(L) - (h_N/3)S_x(L) + \mathcal{O}(h^2) \\ &= S(L - h_N/3) + \mathcal{O}(h^2), \end{aligned}$$

which is independent of ε . For quadratic elements we find

$$\psi(x) = 6 \frac{x - x_l}{h_N} \left[\frac{\varepsilon}{uh_N} \left(2 \frac{x - x_l}{h_N} - 1 \right) + \frac{\varepsilon^2}{u^2 h_N^2} \left(3 \frac{x - x_l}{h_N} - 4 \right) \right]$$

and

$$\alpha = S(L) + \frac{\varepsilon}{u} S_x(L) + \mathcal{O}(h^2 + \varepsilon h),$$

whereas for finite elements of degree p it may be shown that

$$\alpha = S(L) + \frac{\varepsilon}{u} S_x(L) + \dots + \left(\frac{\varepsilon}{u} \right)^{p-1} \frac{\partial^{p-1} S}{\partial x^{p-1}}(L) + \mathcal{O}(h^p + \varepsilon h^{p-1} + \dots + \varepsilon^{p-1} h). \quad (36)$$

In order to relate the implied boundary condition $uT_x = \alpha$ to the solution of the original problem on the semi-infinite real line, we note that the exact solution T^∞ satisfies the differential equation

$$T_x^\infty - \frac{\varepsilon}{u} T_{xx}^\infty = \frac{1}{u} S$$

on $0 < x < \infty$ and multiplying both sides by the differential operator

$$1 + \frac{\varepsilon}{u} \frac{\partial}{\partial x} + \dots + \left(\frac{\varepsilon}{u} \right)^{p-1} \frac{\partial^{p-1}}{\partial x^{p-1}},$$

we find that

$$uT_x^\infty(L) = S(L) + \dots + \left(\frac{\varepsilon}{u} \right)^{p-1} \frac{\partial^{p-1} S}{\partial x^{p-1}}(L) + u \left(\frac{\varepsilon}{u} \right)^p \frac{\partial^{p+1} T^\infty}{\partial x^{p+1}}(L) \quad (37)$$

provided that S is sufficiently smooth. Thus, in the limit $h \rightarrow 0$,

$$uT_x^\infty(L) = \alpha + u \left(\frac{\varepsilon}{u} \right)^p \frac{\partial^{p+1} T^\infty}{\partial x^{p+1}}(L),$$

so that the BC $uT_x(L) = \alpha$ is equivalent, in this limit, to the BC $\partial^{p+1} T / \partial x^{p+1} = 0$ used in (23) (see also (4) with $j = p + 1$).

It now follows that the difference $e = T^\infty - T$, where T is a solution of (35), satisfies

$$\begin{aligned} -\varepsilon e_{xx} + u e_x &= 0, & 0 < x < L \\ e(0) &= 0, \\ u e_x(L) &= \delta, \end{aligned}$$

where $\delta = \mathcal{O}((\varepsilon + h)^p)$. By the same reasoning that led to Lemma 1, we may conclude that

$$T^\infty - T = \mathcal{O}(\varepsilon(\varepsilon + h)^p).$$

The standard Galerkin method will, subject to smoothness of the data, generate a numerical solution T^h that is within $\mathcal{O}(h^{p+1})$ of T . Consequently,

$$T^\infty - T^h = \mathcal{O}(\varepsilon(\varepsilon + h)^p + h^{p+1}). \tag{38}$$

The error is therefore $\mathcal{O}(h^{p+1})$ when $\varepsilon \ll h$ and $\mathcal{O}(\varepsilon^{p+1})$ when $h \ll \varepsilon$, which is exactly the behaviour found in Example 1 (see Figures 3 and 4).

The same construction applies to unsteady problems and may be shown to lead to the IBVP

$$\begin{aligned} T_t + uT_x &= \varepsilon T_{xx} + S, & 0 < x < L, \\ T(0, t) &= 0, \\ uT_x(L, t) &= \alpha, \end{aligned}$$

where

$$\alpha = \frac{u}{\varepsilon} \int_{x_l}^L \psi(S - T_t) ds$$

and ψ retains its earlier definition. To reduce the amount of detail, we assume that S is a polynomial of degree p in x (or that it is interpolated into the finite element basis) and discuss the cases $p = 1$ and 2.

For $p = 1$ it may be shown that the BC $uT_x(L, t) = \alpha$ may be written as

$$T_t + uT_x = S - \frac{1}{3} h_N(S_x - T_{xt})$$

at $x = L$, so that as $h \rightarrow 0$ we obtain the condition $T_t + uT_x = S$ (cf (3)), which is equivalent to setting $T_{xx}(L, t) = 0$.

For $p = 2$ the corresponding BC is

$$T_t + uT_x = S - \frac{\varepsilon}{u}(S_x - T_{xt}) - \frac{1}{20} h_N^2(S_{xx} - T_{xxt}). \tag{39}$$

By differentiating (1) and eliminating T_{xx} , it may be shown that T^∞ satisfies

$$T_t^\infty + uT_x^\infty = S - \frac{\varepsilon}{u}(S_x - T_{xt}^\infty) - u\left(\frac{\varepsilon}{u}\right)^2 T_{xxx}^\infty$$

and we see that in the limit $h \rightarrow 0$ the implied BC (39) for quadratic elements is equivalent to setting $T_{xxx}(L, t) = 0$.

A similar approach may be adopted for $p > 2$ to show that the ‘no BC’ finite element equations converge to the Galerkin finite element approximation of (1) on $0 < x < L$ with the ‘extrapolation’ boundary condition $\partial^{p+1}T/\partial x^{p+1} = 0$ at $x = L$.

We believe that the arguments used in this section may be extended to higher dimensions and this will be reported on in a future paper.

ACKNOWLEDGEMENTS

We would like to thank Dr. Bosco García Archilla for supplying the Matlab routines used for time integration and Dr. Phil Gresho for not only introducing us to these boundary conditions but also for his continued interest in the work.

REFERENCES

1. J.-P. Lohéac, 'An artificial boundary condition for an advection–diffusion equation', *Math. Methods Appl. Sci.*, **14**, 155–175 (1991).
2. B. C. V. Johansson, 'Boundary conditions for open boundaries for the incompressible Navier–Stokes equation', *J. Comput. Phys.*, **105**, 233–251 (1993).
3. J. Nordström, 'Accurate solutions of the Navier–Stokes equations despite unknown outflow boundary data', *J. Comput. Phys.*, **120**, 184–205 (1995).
4. N. T. Malamataris and T. C. Papanastasiou, 'Unsteady free surface flows on truncated domains', *Indian J. Chem. Res.*, **30**, 2211 (1991).
5. T. C. Papanastasiou, M. Malamataris and K. Ellwood, 'A new outflow boundary condition', *Int. j. numer. methods fluids*, **14**, 587–608 (1992).
6. R. L. Sani and P. M. Gresho, 'Résumé and remarks on the Open Boundary Condition Minisymposium', *Int. j. numer. methods fluids*, **18**, 983–1008 (1994).
7. J. C. Heinrich and C. A. Vionnet, 'On boundary conditions for unbounded flows', *Commun. Numer. Methods Eng.*, **11**, 179–186 (1995).
8. P. J. Davis and P. Rabinowitz, *Methods of Numerical Integration*, 2nd edn, Academic, New York, 1984.
9. H.-O. Kreiss and J. Oliger, *Methods for the Approximate Solution of Time Dependent Problems*, World Meteorological Organization, Geneva, 1973.
10. J. C. Strikwerda, *Finite Difference Schemes and Partial Differential Equations*, Wadsworth & Brooks, Pacific Grove, CA, 1989.